

Electric Dipole Transition of the First Excited State of ${}^9\text{Be}$

M.Odsuren^{1,2,*}, K.Katō³, G.Khuukhenkhuu^{1,2}, S.Davaa^{1,2}

¹*School of Engineering and Applied Sciences, National University of Mongolia, Ulaanbaatar, Mongolia*

²*Nuclear Research Center, National University of Mongolia, Ulaanbaatar, Mongolia*

³*Nuclear Reaction Data Centre, Faculty of Science, Hokkaido University, Sapporo, Japan*

The E1 transition strength of the $1/2^+$ first excited state of ${}^9\text{Be}$ is calculated using three body cluster model and complex scaling method where the excited state is correctly treated as unbound. The $1/2^+$ resonance is obtained using the attractive three-body potential.

PACS numbers: 27.20.+n, 6.56.Az, 21.60.Gx, 24.30.Gd, 25.20.Lj

Keywords: light nuclei, electric dipole transition, potential strength

INTRODUCTION

It is a longstanding problem to determine resonance energy and decay width of the first excited $1/2^+$ state of ${}^9\text{Be}$, which is closely connected with the problem to clarify whether it is a resonant state or not. The resonant structure [1-5] and a virtual characteristic state [6] of ${}^9\text{Be}(1/2^+)$ have been studied by the various theoretical approaches and photo-dissociation experiments. However, a complete understanding on the nature of ${}^9\text{Be}(1/2^+)$ state has not yet been obtained. It is desired to perform a more comprehensive study based on an $\alpha+\alpha+n$ three-body calculations which can treat the bound ground state and also the unbound resonant states of ${}^9\text{Be}$ in an unified framework.

The low-energy photodisintegration of ${}^9\text{Be}$ has also received much attention from the viewpoint of the astrophysical interest. The photodisintegration cross section has been discussed to be negligibly small in the energy region between thresholds of $\alpha+\alpha+n$ (1.5736 MeV) and ${}^8\text{Be}+n$ (1.6654 MeV). The observed cross section above the ${}^8\text{Be}+n$ shows a prominent peak, although there are some discrepancies among the experimental absolute values. The cross section profile has an asymmetric shape and cannot be explained by a simple resonance formula like the Breit-Wigner form.

In this work, the complex scaling method (CSM) [7-8] is applied to an $\alpha+\alpha+n$ three-cluster model for understanding the nuclear structure and (γ,n) reactions for low-lying states in ${}^9\text{Be}$.

We treat the unbound nature of the $1/2^+$ state of ${}^9\text{Be}$ and investigate the $E1$ transition between $1/2^+$ and $3/2^-$ states, which contributes to the (γ,n) reaction dominantly. Furthermore, we examine the resonance formation in the (γ,n) reaction to see whether a direct three-body breakup or a two-step process through the ${}^8\text{Be}+n$ intermediate resonant state is dominant.

FRAMEWORK

A. $\alpha+\alpha+n$ three body model

The Schrödinger equation for the $\alpha+\alpha+n$ system using the orthogonality condition model (OCM) is solved. The Schrödinger equation is given as

$$\hat{H} \Psi_{J^\pi}^\nu = E_\nu \Psi_{J^\pi}^\nu \quad (1)$$

where J^π is the total spin and parity of the $\alpha+\alpha+n$ system and ν is the index of eigenstates. The energy eigenvalue E_ν is measured from the $\alpha+\alpha+n$ threshold of ${}^9\text{Be}$. The Hamiltonian for the relative motion of the $\alpha+\alpha+n$ three-body system is given as

$$\hat{H} = \sum_{i=1}^3 t_i - T_{c.m.} + \sum_{i=1}^2 V_{an}(\xi_i) + V_{\alpha\alpha} + V_{PF} + V_3 \quad (2)$$

where t_i and $T_{c.m.}$ are kinetic energy operators for each particle and the center-of mass of the system, respectively. The interaction between the neutron and the i -th α particle is given as $V_{an}(\xi_i)$, where ξ_i is the relative coordinate between them. The Kanada, Kaneko, Nagata, Nomoto (KKNN) potential [9] is employed for V_{an} . For the $\alpha+\alpha$ interaction $V_{\alpha\alpha}$, we employ the same potential as used in Ref. [10], which is a folding potential of the effective nucleon-nucleon (NN) interaction and the Coulomb interaction.

The pseudopotential $V_{PF} = \lambda |\Phi_{PF}\rangle\langle\Phi_{PF}|$ is the projection operator to remove the Pauli forbidden states from the relative motions of $\alpha+\alpha$ and $\alpha+n$. The Pauli forbidden state Φ_{PF} is defined as the harmonic oscillator wave functions by assuming the $(0s)^4$ configuration, whose oscillator length ($\lambda=10^6$ MeV) is fixed to

* Electronic address: odsurenn@gmail.com

reproduce the observed charge radius of the α particle. In the present calculation, the $\alpha+\alpha+n$ three-body potential V_3 is used. The explicit form of V_3 is given as

$$V_3 = v_{3b} \exp(-\mu\rho^2) \quad (3)$$

where ρ is the hyper-radius of the $\alpha+\alpha+n$ system. The hyper-radius is defined as

$$\rho^2 = 2r^2 + \frac{8}{9}R^2,$$

where r is the distance between two α 's and R is that between the neutron and the center-of-mass of the α - α subsystem. To reproduce the ground-state properties, we take the potential strength v_{3b} and the potential width μ as 1.10 MeV and 0.02 fm^{-2} , respectively. For other spin-parity states, the same value of μ as used in $3/2^-$ states is employed, and different strengths are used to reproduce the energy positions of the observed peaks in the photodisintegration cross section.

The Schrödinger equation with the coupled rearrangement-channel Gaussian expansion method [11] is solved. In the present calculation, the ${}^9\text{Be}$ wave function $\Phi_{J^\pi}^\nu$ is described in the Jacobi coordinate system as

$$\Phi_{J^\pi}^\nu = \sum_{cij} C_{cij}^\nu (J^\pi) \left[\left[\phi_i^i(r_c) \phi_L^j(\mathbf{R}_c) \right]_1, \chi_{\frac{1}{2}} \right]_{J^\pi} \quad (4)$$

where $C_{cij}^\nu(J^\pi)$ is a expansion coefficient and $\chi_{\frac{1}{2}}$ is the spin wave function. The relative coordinates r_c and \mathbf{R}_c are those in three kinds of the Jacobi coordinate systems indexed by c ($= 1, 2, 3$), and the indices for the basis functions are represented as i and j . The spatial part of the wave function is expanded with the Gaussian basis functions.

B. Complex scaling method

To calculate the photodisintegration cross section, we use the CSM [7-8,10]. In the CSM, the relative coordinates ξ (r_c and \mathbf{R}_c) are transformed as

$$U(\theta)\xi U^{-1}(\theta) = \xi e^{i\theta}, \quad (5)$$

where $U(\theta)$ is a complex scaling operator and θ is a scaling angle being a real number. Applying this transformation to Eq. (1), the complex scaled Schrödinger equation is obtained as

$$\hat{H}^\theta \Psi_{J^\pi}^\nu(\theta) = E_\nu^\theta \Psi_{J^\pi}^\nu(\theta). \quad (6)$$

By solving the complex-scaled Schrödinger equation with appropriate \mathcal{L}^2 basis functions, we

obtain the energy eigenvalues E_ν^θ and eigenstates $\Psi_{J^\pi}^\nu(\theta)$ (their biorthogonal states $\tilde{\Psi}_{J^\pi}^\nu(\theta)$) [10].

The energy eigenvalues E_ν^θ obtained on the complex energy plane are governed by the Aguilar, Balslev, Combes (ABC) theorem [7-8]. A schematic picture of the energy eigenvalue distribution is shown in Fig. 1.

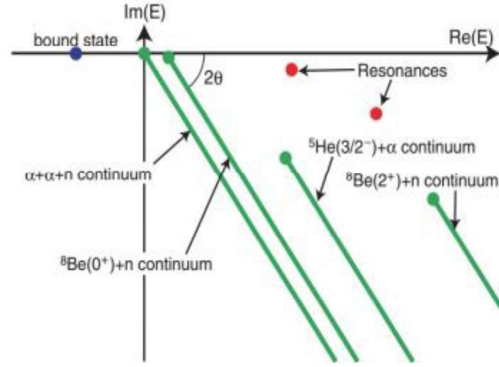


Figure 1: Schematic picture of energy eigenvalue distribution on the complex energy plane for the $\alpha+\alpha+n$ system.

In the CSM, the energies of bound states are given by real numbers and are invariant under the complex scaling. On the other hand, resonances and continuum states are obtained as eigenstates with complex energy eigenvalues. The resonances are obtained as isolated eigenstates on the complex energy plane, whose energies are given as $E_\nu^\theta = E_\nu^r - i\Gamma_\nu/2$. The resonance energies E_ν^r and the decay widths Γ_ν are independent of the scaling angle θ . The complex-scaled continuum states are obtained on branch cuts rotated down by 2θ as shown in Fig. 1.

The branch cuts start from the different thresholds for two- and three-body continuum states in the case of the $\alpha+\alpha+n$ system as shown in Fig. 1. This classification of the continuum states is useful in investigation of properties of the ${}^9\text{Be}$ photodisintegration.

Using the energy eigenvalues and eigenstates of the complex-scaled Hamiltonian \hat{H}^θ , the complex-scaled Green's function is defined as

$$\mathcal{G}^\theta(E; \xi, \xi') = \langle \xi | \frac{1}{E - \hat{H}^\theta} | \xi' \rangle = \sum_\nu \frac{\Psi_{J^\pi}^\nu(\theta) \tilde{\Psi}_{J^\pi}^\nu(\theta)}{E - E_\nu^\theta} \quad (7)$$

In the derivation of the right-hand side of Eq. (7), we use the extended completeness relation. The cross section is calculated

$${}^9\text{Be}(3/2^-) + \gamma \rightarrow \alpha + \alpha + n,$$

in terms of the electric-dipole transition. In the present calculation, we focus on the low-lying region of the photodisintegration cross section and take into account only the dipole responses.

The photodisintegration cross section σ is given by the $E1$ ransition as

$$\sigma^\gamma(E_\gamma) = \sigma_{E1}(E_\gamma), \quad (8)$$

where E_γ is the incident photon energy. The energy E in Eq. (7) is related to E_γ as $E = E_\gamma - E_{g.s.}$ where $E_{g.s.}$ is the binding energy of the ${}^9\text{Be}$ ground state measured from the $\alpha+\alpha+n$ threshold. The cross sections for the electric-dipole transition σ_{E1} are expressed as the following form:

$$\sigma_{E1}(E_\gamma) = \frac{16\pi^3}{9} \left(\frac{E_\gamma}{hc} \right) \frac{dB(E1, E_\gamma)}{dE_\gamma}. \quad (9)$$

Using the CSM and the complex-scaled Green's function in Eq. (7), the electric-dipole transition strength is given as

$$\begin{aligned} & \frac{dB(E1, E_\gamma)}{dE_\gamma} \\ &= -\frac{1}{\pi} \frac{1}{2J_{g.s.} + 1} \text{Im} \left[\sum_{\nu} \langle \tilde{\Psi}_{g.s.}^{\nu}(\theta) || \hat{O}_{E1}^{\theta} || \Psi^{\nu}(\theta) \rangle \right] \\ & \quad \times \frac{1}{E - E_{\theta}^{\nu}} \langle \tilde{\Psi}^{\nu}(\theta) || \hat{O}_{E1}^{\theta} || \Psi_{g.s.}(\theta) \rangle. \end{aligned} \quad (10)$$

Where $J_{g.s.}$ and $\Psi_{g.s.}(\theta)$ are the total spin and the wave function of the ground state, respectively, and \hat{O}_{E1}^{θ} is an electric-dipole transition operator.

RESULTS AND DISCUSSION

The $3/2^-$ ground state of ${}^9\text{Be}$ is calculated at 2.16 MeV from the $\alpha+\alpha+n$ threshold with no three-body potential ($v_3 = 0$) by M.Kato [12]. The two-cluster potentials $V_{\alpha n}$ and $V_{\alpha\alpha}$ are fixed to reproduce the experimental data of the corresponding subsystems. Here, we introduce a repulsive three-body potential

$v_{3b} = 1.10 \text{ MeV}$, $\mu = 0.02 \text{ fm}^{-2}$) to fit the observed binding energy (-1.574 MeV) of ${}^9\text{Be}$.

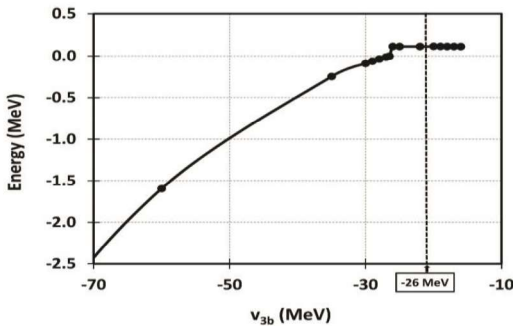


Figure 2. Energies of the $1/2^+$ state measured from the $\alpha+\alpha+n$ threshold, as a function of the three-body potential strength v_{3b} .

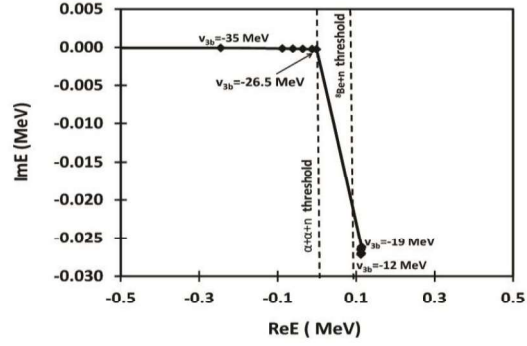


Figure 3. The eigenvalue trajectory of the $1/2^+$ state in the complex-energy plane.

The Hamiltonian Eq.(2) reproduces all the threshold energies of $\alpha+\alpha+n$, ${}^8\text{Be}+n$ and ${}^5\text{He}+\alpha$ in the ${}^9\text{Be}$ nucleus. Using this Hamiltonian, we do not obtain the $1/2^+$ resonance of ${}^9\text{Be}$. This result is the same as that obtained in Refs. [6, 12].

To clarify the resonance nature of the $1/2^+$ state, we carry out three-body calculation of the $1/2^+$ state by adding the three-body potential. With a strong attractive three-body potential with a negative value of v_{3b} , the $1/2^+$ state is obtained as a bound state as shown in Fig. 2.

From calculations for various values of v_{3b} , we find that the $1/2^+$ state becomes bound with the value of v_{3b} below -26 MeV. Increasing the value of v_{3b} from -26 MeV gradually, we search for the $1/2^+$ resonance solutions in the CSM, whose eigenvalue trajectory is shown in Fig. 3. It can be seen that there is a jump from the $\alpha+\alpha+n$ threshold energy to a complex value, the real part of which corresponds to a energy just above the ${}^8\text{Be}+n$ threshold. This discontinuity of the trajectory may be understood by considering the properties of solutions in the CSM.

In the CSM, resonance poles existing below the 2θ line of continuum states starting from the lowest threshold of $\alpha+\alpha+n$ cannot be obtained as isolated eigenvalues. Because of the analyticity condition for the present complex scaled Hamiltonian, the θ value must be smaller than 45° [7].

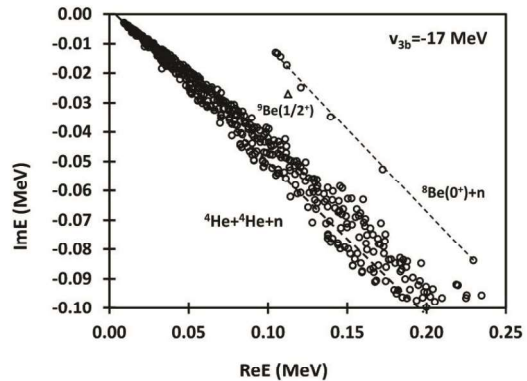


Figure 4. The $1/2^+$ energy eigenvalue distribution in the complex energy plane for the $\alpha+\alpha+n$ model.

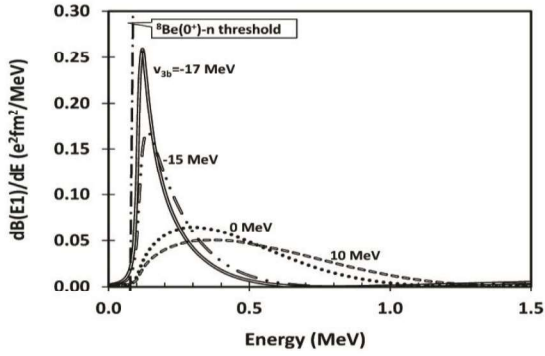


Figure 5. The $E1$ transition strength for ${}^9\text{Be}$ ($3/2^-$ to $1/2^+$) as a function of energy E , changing the strength v_{3b} of the three-body potential.

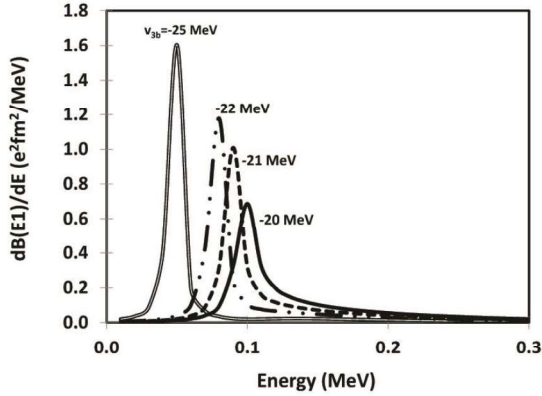


Figure 6. The $E1$ transition strength ${}^9\text{Be}$ ($3/2^-$ to $1/2^+$) calculated for $v_{3b} = -20, -21, -22, -25$ MeV.

For virtual states (whose energy eigenvalue is located at the negative real axis of the second Riemann surface), the angle θ has to be larger than 90° . When a virtual state exists in the ${}^8\text{Be}+n$ channel, a jump is expected in the resonance trajectory as discussed in Ref. [13]. The present case is not a two-body system but the $\alpha+\alpha+n$ three-body one. It is difficult to trace the jump behavior of the pole solutions in the CSM.

Fig. 4 displays an example of the eigenvalue distribution of ${}^9\text{Be}(1/2^+)$ for $v_{3b} = 17$ MeV with $\theta = 15^\circ$. Besides the triangle corresponding to the resonance, all solutions for continuum states described by open circles lie on two straight lines starting from positions of the $\alpha+\alpha+n$ three- and ${}^8\text{Be}(0^+)+n$ two-body thresholds. To investigate the effect of the $1/2^+$ resonance of ${}^9\text{Be}$, the $E1$ transition strength is calculated by using the solutions of the $1/2^+$ state and the ground state.

In Fig. 5, the results are shown as a function of the energy measured from the $\alpha+\alpha+n$ threshold for several values of the three-body potential strength v_{3b} . The $v_{3b} = -15$ and -17.1 MeV (attractive) or the $v_{3b} = 0$ and 10 MeV (repulsive) three-body potential strengths are applied. The $E1$ transition strength for $v_{3b} = -17.1$ MeV rises sharply from

the ${}^8\text{Be}(0^+)+n$ two-body threshold. The transition strength reaches with a maximum of 0.26 $\text{e}^2\text{fm}^2/\text{MeV}$ at $E=0.11$ MeV, and decreases to 0.01 $\text{e}^2\text{fm}^2/\text{MeV}$ at $E=0.5$ MeV. As v_{3b} increases, the peaks of the $E1$ transition strength decrease gradually and move into higher energies. In the cases of $v_{3b} = 0$ and 10 MeV, the peaks of the $E1$ strength are broad and their energy positions are distant from the ${}^8\text{Be}(0^+)+n$ threshold. It is noted that the $E1$ transition strength is very small in the energy region below the ${}^8\text{Be}(0^+)+n$ two-body threshold.

The $E1$ transition strengths calculated for $v_{3b} = -20 \sim -25$ MeV are shown in Fig. 6. They have transition strengths in the energy region between $\alpha+\alpha+n$ and the ${}^8\text{Be}(0^+)+n$ thresholds. Each $E1$ transition strength seems to be expressed by the Breit-Wigner form. In the case of $v_{3b} < -25$ MeV, where the $1/2^+$ state becomes a bound state, the $E1$ transition strengths have not a characteristic structure around $\alpha+\alpha+n$ and ${}^8\text{Be}(0^+)+n$ threshold energies.

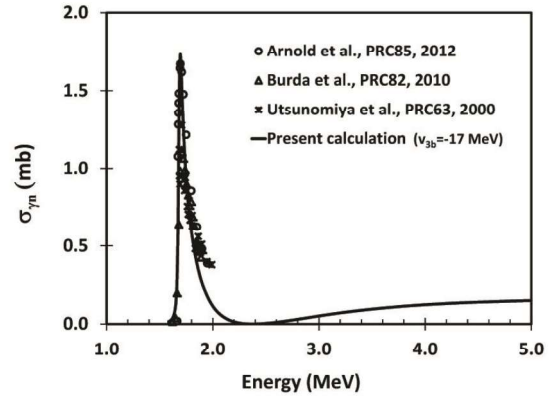


Figure 7. The ${}^9\text{Be}(\gamma, n){}^8\text{Be}$ cross section σ_m as a function of excitation energy E . The experimental data are taken from Refs. [1-3]

Comparing the calculated photo-disintegration cross section of the $1/2^+$ state with the recent new experiment [1], we find that $v_{3b} = -17.1$ MeV gives a good agreement as shown in Fig. 7. Using this v_{3b} we obtain $1/2^+$ as a three-body resonance. This result indicates that the experimental cross section can be explained in terms of the $1/2^+$ resonance of ${}^9\text{Be}$.

SUMMARY

In this work, the properties of the $1/2^+$ state of ${}^9\text{Be}$ with varying values of three-body potential are studied. Without the three-body potential, we cannot obtain the $1/2^+$ resonance of ${}^9\text{Be}$, which is consistent to the results in Refs. [6, 12]. The $1/2^+$ resonance is obtained using the attractive three-body potential, which is responsible to explain the $E1$ transition strength of ${}^9\text{Be}$ with an enhancement near the $\alpha+\alpha+n$

threshold energy. The calculated photo-disintegration cross section is in good agreement with new experimental data [1] using the resonance solution of ${}^9\text{Be}(1/2^+)$ with an appropriate strength of the three-body potential.

ACKNOWLEDGEMENTS

The numerical calculations were done with use of computing system of the Nuclear Research Center, National University of Mongolia.

REFERENCES

- [1] C.W.Arnold, T.B.Clegg, C.Iliadis, H.J.Karwowski, G.C.Rich, J.R.Tompkins, C.R.Howell, Cross-section measurement of ${}^9\text{Be}(\gamma, n){}^8\text{Be}$ and implications for $\alpha+\alpha+n\rightarrow{}^9\text{Be}$ in the r process, *Phys. Rev. C* **85**, 044605, (2012)
- [2] O.Burda, P. von Neumann-Cosel, A.Richter, C.Forssen, B.A.Brown, Resonance parameters of the first $1/2^+$ state in ${}^9\text{Be}$ and astrophysical implications, *Phys. Rev. C* **82**, 015808, (2010)
- [3] H.Utsunomiya, Y.Yonezawa, H.Akimune, T.Yamagata, M.Ohta, M.Fujishiro, H.Toyokawa, H.Ohgaki, Photodisintegration of ${}^9\text{Be}$ with laser-induced Compton backscattered γ rays, *Phys. Rev. C* **63**, 018801, (2000)
- [4] V.D.Efros, P. von Neumann-Cosel, A.Richter, Resonance parameters of the first $1/2^+$ state in ${}^9\text{Be}$ and astrophysical implications, *Phys. Rev. C* **89**, 027301, (2010)
- [5] E.Gariddo, D.V.Fedorov, A.S.Jensen, Above threshold s-wave resonances illustrated by the $1/2^+$ states in ${}^9\text{Be}$ and ${}^9\text{Be}$, *Phys. Lett. B* **684**, 132, (2010)
- [6] K.Arai, P.Descouvemont, D.Baye, W.N.Catford, Resonance structure of ${}^9\text{Be}$ and ${}^9\text{B}$ in a microscopic cluster model, *Phys. Rev. C* **68**, 014310, (2003)
- [7] S.Aoyama, T. Myo, K.Kato, K.Ikeda, The complex scaling method for many-body resonances and its applications to three-body resonances, *Prog. Theor. Phys.* **116**, 1, (2006)
- [8] T.Myo, K.Kato, S.Aoyama, K.Ikeda, Analysis of ${}^6\text{He}$ coulomb breakup in the complex scaling method, *Phys. Rev. C* **63**, 054313, (2001)
- [9] H.Kanada, T.Kaneko, S.Nagata, M.Nomoto, Microscopic study of nucleon- ${}^4\text{He}$ scattering and effective nuclear potentials, *Prog. Theor. Phys.* **61**, 1327, (1979)
- [10] M.Odsuren, K.Kato, M.Aikawa, T. Myo, Decomposition of scattering phase shifts and reaction cross sections using the complex scaling method, *Phys. Rev. C* **89**, 034322, (2014)
- [11] E.Hiyama, Y.Kino, M.Kamimura, Gaussian expansion method for few-body systems, *Prog. Part. Nucl. Phys.* **51**, 223, (2003)
- [12] M.Kato, Investigation of ${}^9\text{Be}$ in the complex scaling method, Master Thesis in Hokkaido University (March, 2012) and private communication.
- [13] H.Masui, S.Aoyama, T.Myo, K.Kato, K.Ikeda, Study of virtual states in ${}^5\text{He}$ and ${}^{10}\text{Li}$ with the jost function method, *Nucl. Phys. A* **673**, 207 (2000).